Journal of Alloys and Compounds 489 (2010) 714–718

Contents lists available at ScienceDirect

Journal of Alloys and Compounds

journal homepage: www.elsevier.com/locate/jallcom

Study of $LiMgVO_4$ electrical conductivity mechanism

C. Paraskeva[a], A. Kazakopoulos[b], K. Chrissafis[a], O. Kalogirou[a,*]

[a] Department of Physics, Aristotle University of Thessaloniki, 54 124 Thessaloniki, Greece
[b] Department of Electronics, T.E.I. of Thessaloniki, 57 400 Thessaloniki, Greece

ARTICLE INFO

Article history:
Received 1 July 2009
Received in revised form
24 September 2009
Accepted 27 September 2009
Available online 9 October 2009

Keywords:
$LiMgVO_4$
Impedance spectroscopy
Ionic conductivity
Humidity sensors

ABSTRACT

This paper deals with impedance spectroscopy on single-phase polycrystalline $LiMgVO_4$ in the temperature range of 25–500 °C. Thermogravimetric measurements show a weight loss of 2.7% in the temperature range between 25 °C and 175 °C due to humidity desorption. A conductivity mechanism along the grain boundaries (agb) is identified in the specific temperature range and is attributed to a reversible humidity absorption–desorption mechanism. Equivalent circuits are drawn using the results of the impedance measurements at each temperature. A unique conduction process within the material is assigned to each element of the equivalent circuit and Arrhenius plots are plotted. The calculation of activation energy of each conduction mechanism is based on the Arrhenius plots. The activation energy E_b of the bulk conductivity mechanism was found to be 0.62 eV. The activation energy E_{gb} of the grain boundaries conductivity mechanism was found to be 1.03 eV up to 275 °C and 0.50 eV in the temperature range of 300–500 °C. The absence of the conductivity mechanism along the grain boundaries above 175 °C can only be due to the complete removal of water from the material's grains.

1. Introduction

The first studies of $LiMgVO_4$ have been published by Blasse [1,2], who proposed an olivine structure and gave unit cell parameters based on the olivine space group D_{2h}^{16}. In Ref. [3] Paques-Ledent has shown that the X-ray powder diffraction diagram does not agree with the olivine structure. In a later paper [4] Paques-Ledent has proposed that $LiMgVO_4$ is a vanadate isomorph with Na_2CrO_4-type structure. In Ref. [5] Capsoni et al. have studied the cation distribution in $LiMgVO_4$ and $LiZnVO_4$ and obtained the room temperature cation occupancy in $LiMgVO_4$ and $LiZnVO_4$ crystallographic sites by means of the combined use of X-ray powder diffraction, ^7Li and ^{51}V magic angle spinning nuclear magnetic resonance (MAS NMR) and micro-Raman measurements. Interesting properties have been reported related to the luminescence which is due to the tetrahedrally coordinated V^{5+} ions [6–8].

In the category of $LiMVO_4$ materials, where M = Cu, Ni, Co, Zn, Cd, Mg, Be and Li, special attention has been paid to $LiNiVO_4$ and $LiCoVO_4$ that have an inverse spinel structure and can be reversibly lithiated [9]. In Ref. [10] we have reported an impedance analysis study on $LiNiVO_4$ and $LiCoVO_4$ and showed that a reversible water absorption–desorption mechanism over the temperature range of 25–150 °C is responsible for the behavior of the materials between the above temperatures, which is not consistent with pure ionic conductivity. A similar behavior has been found in the case of Li_3VO_4 [11] but not in the case of $LiCuVO_4$, where no water absorption has been observed [12]. In Ref. [10] it was also shown that the amount and rate of water absorption depends on microstructure of the compound and air exposure conditions. Most likely, for these materials, there exists a conduction mechanism along the grain boundaries (agb), caused by humidity. The electrical properties of $LiMgVO_4$ have not yet been reported as far as we know. As it is discussed below, the study of the electrical properties of $LiMgVO_4$ and especially the effect of humidity on its conductivity is of particular interest, since it may lead to the possibility of its use as a humidity sensor like $LiZnVO_4$ [13–15]. As a matter of fact, it is the dramatic change in conductivity due to the humidity of the surrounding atmosphere (up to seven orders of magnitude as shown below), which could be exploited in humidity sensor applications. In this paper, for the first time, we report on the conduction mechanisms of polycrystalline $LiMgVO_4$ in the temperature range of 25–500 °C by means of impedance spectroscopy measurements. It is shown that, humidity strongly affects the electric performance of $LiMgVO_4$ too, which strengthens our interpretation used in the case of $LiNiVO_4$, $LiCoVO_4$ and Li_3VO_4 [10,11].

2. Experimental

Polycrystalline $LiMgVO_4$ was prepared with conventional solid-state reaction as described in Ref. [9].

$$Li_2CO_3 + 2MgO + 2NH_4VO_3 \xrightarrow{650\,^\circ C,4days} 2LiMgVO_4 + 2NH_3 + H_2O + CO_2$$

* Corresponding author. Tel.: +30 2310 998148; fax: +30 2310 998003.
E-mail address: orestis.kalogirou@physics.auth.gr (O. Kalogirou).

0925-8388/$ – see front matter © 2009 Elsevier B.V. All rights reserved.
doi:10.1016/j.jallcom.2009.09.159

Chemical characterization of the material was accomplished by using electron microprobe (EDAX). Photographs taken by scanning electron microscopy (SEM) were used to study its morphology. X-ray powder diffraction (XRD) using Cu $K\alpha_1$ radiation was used to confirm the structure. SETARAM SETSYS TG/DTA equipment was used to carry out thermogravimetric measurements. Impedance data was collected on cylindrical pellets (~16 mm in diameter with a thickness of 2 mm), obtained by applying pressure of 5 ton/cm^2 for 30 s in a 16 mm die. The density of the samples was found to be 83% of the crystallographic density. Nickel plate electrodes were used. An impedance analyzer HIOKI 3532-50 was used over the frequency range of 42 Hz to 1 MHz to collect the impedance data. Initially, measurements were carried out in order to examine whether the material displays a linear behavior. It was found that the material displays a linear behavior when the applied voltage is above 150 mV. All measurements were taken by applying a constant voltage of 200 mV. The impedance of the pellets was measured at frequencies 50 Hz, 100 Hz, 1 KHz, 10 KHz, 100 KHz and 1 MHz, as the pellet was being heated up to 500 °C at a rate of 50 °C/h and then cooled down to room temperature. These measurements were taken in order to check the reproducibility and hysteresis phenomena. The impedance of the samples was measured at 100 different frequency values, logarithmically distributed in the range from 42 Hz to 10^6 Hz, at temperatures from 25 °C to 500 °C, in 25 °C steps. During the measurements a constant pressure was applied, using an adjustable spring mechanism on the electrode-sample system. When the desired temperature was reached, there was a delay of 1 h until impedance measurements were taken. During this stabilization time the temperature varied less than 1 °C.

3. Results and discussion

The proportion of atoms indicated by electron microprobe was the same with the proportion predicted by the chemical formula of the compound, with the exception of Li, the proportion of which could not be calculated because of its low atomic number. From the SEM photographs of the compound it was estimated that the diameter of the grains ranges between 10 μm and 40 μm (Fig. 1). The XRD pattern of the prepared powder (Fig. 2) shows that no additional lines were found that could be assigned to the presence of impurities. The XRD pattern confirms the presence of a single-phase $LiMgVO_4$ (PDF #380275).

The plots in Fig. 3 indicate that at each temperature level there is a frequency which corresponds to the hopping rate. Above this frequency the conductivity is a linear function of frequency in the $\log(\sigma)$ versus $\log(f)$ plots. Therefore the conductivity is expressed above the hopping frequency by a power law expression $\sigma(f) = Af^s$, $0 < s < 1$ [16]. The hopping frequency f_p, which is shown at each temperature level in Fig. 3, corresponds to the frequency at which the conductivity dispersion starts. As it is shown in Fig. 3, below the hopping frequency the conductivity is almost independent from frequency at any given temperature. The impedance measurements taken at 25, 100, 200, 300, 400 and 500 °C are shown in Fig. 4. The results of the impedance measurements were fitted and the equivalent circuits were drawn in 25° intervals, from room temperature to 500 °C, using the EQUIVCRT.PAS program [17]. The equivalent circuits mentioned above at 25 °C, 100 °C, 200 °C, 300 °C, 400 °C and 500 °C and the corresponding fitting results are shown in Fig. 4. The plots drawn during the heating and cooling cycle have the same shape, indicating the same conduction mechanisms during heating and cooling. At higher temperatures hysteresis is negligible but in the low temperature region some hysteresis was observed. A slow heating and cooling rate (50 °C/h) was used between subsequent temperature levels and the sample was kept for 1 h at each temperature level before the measurement was recorded. As our measurements were taken in air atmosphere the material was able to reabsorb a large portion of humidity that had been lost during the heating cycle. The equivalent circuits which were used to fit the measurement results, using the EQUIVCRT.PAS program, consisted of $(R//Q)$ elements in series together with a capacitance C_{dl}, and a Q_{dl} element, the origin of which is described below. The capacitance C_{dl}, named the double-layer capacitance, represents the geometric capacity between the nickel plates and the pellet and was calculated to be in the order of 10^{-1} F/cm in the whole temperature range of 25–500 °C. In the temperature range of 25–175 °C the results were fitted using an equivalent circuit, which consisted of three $(R//Q)$ elements in series. The methodology used to assign the different conductivity processes was the same with that used in the case of $LiNiVO_4$ and $LiCoVO_4$, as it is described in Ref. [10]. The bulk conductivity is represented by the first $(R//Q)$

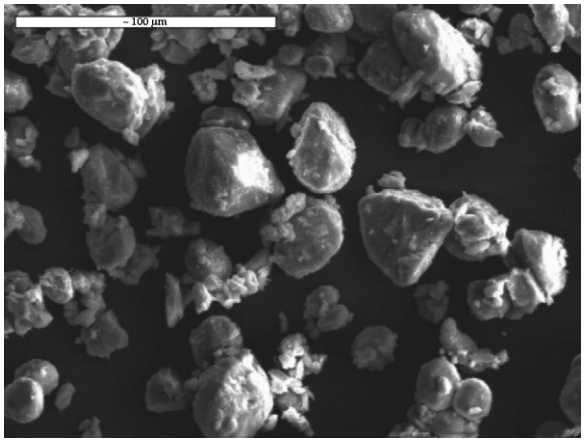

Fig. 1. SEM photograph of $LiMgVO_4$.

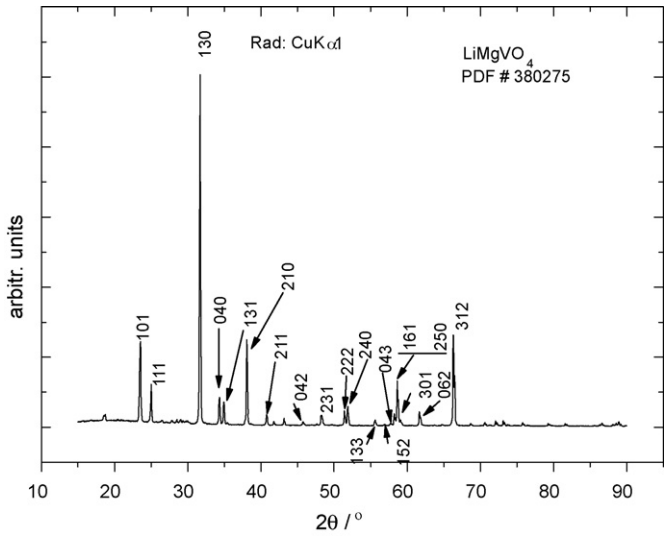

Fig. 2. XRD pattern of $LiMgVO_4$.

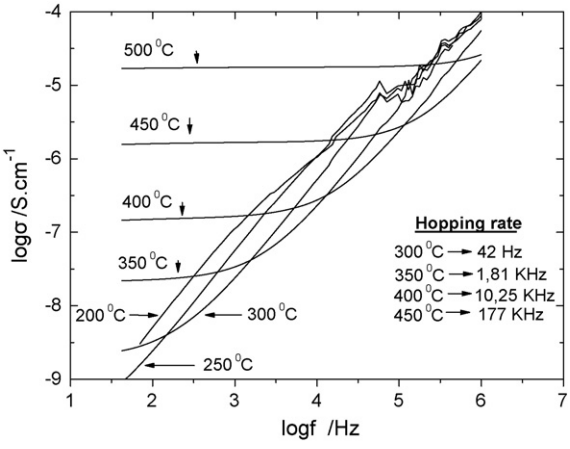

Fig. 3. Log–log plot of the specific conductivity versus frequency at different temperature levels.

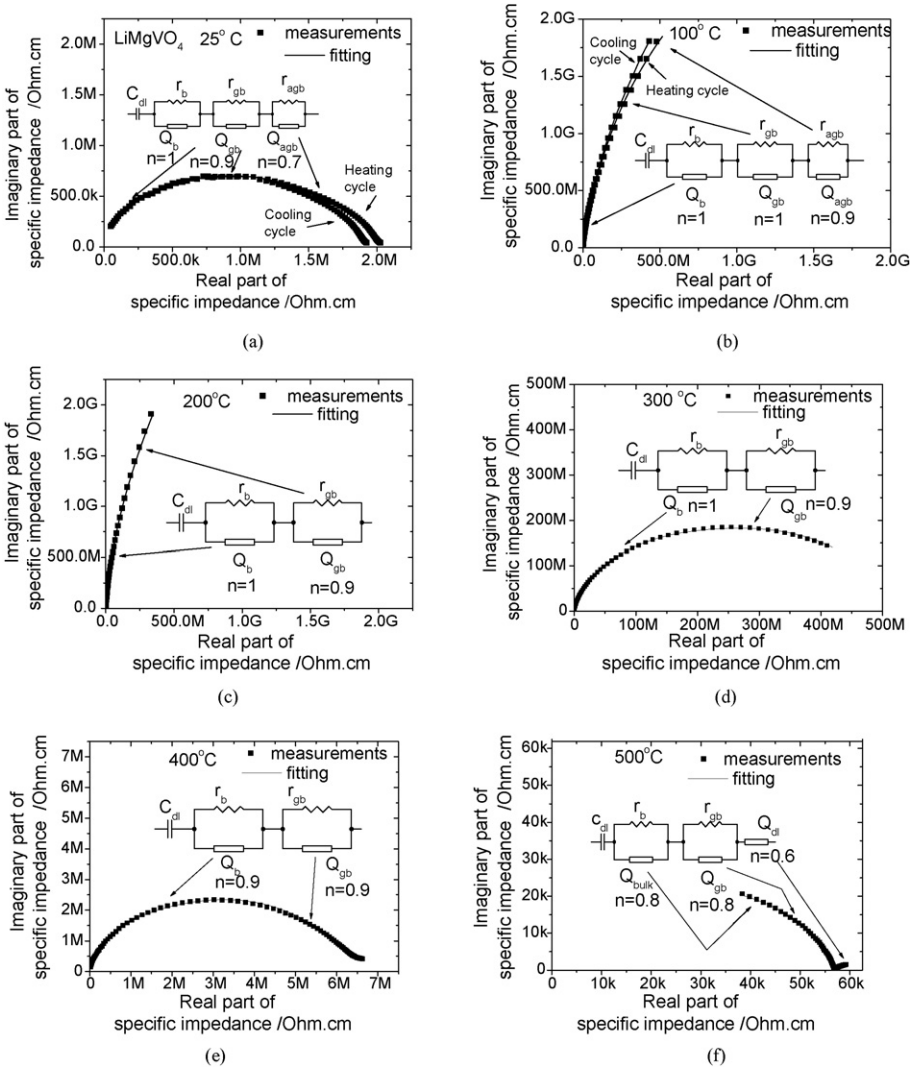

Fig. 4. Imaginary versus real part of the specific impedance, in the frequency range from 42 Hz to 1 MHz, at temperatures (a) 25, (b) 100, (c) 200, (d) 300, (e) 400 and (f) 500 °C; equivalent circuits drawn at each of these temperatures and fitting curves.

element, the grain boundary conductivity is represented by the second ($R//Q$) element and the along the grain boundaries conductivity mechanism was attributed to the third ($R//Q$) element. This assignment was based on time constant arguments [18]. According to these arguments the conductivity process with the smaller time constant was attributed to the along the grain boundaries conductivity. The equivalent circuit that was used to fit the measurement results between 200 °C and 400 °C consists of two ($R//Q$) elements in series, that were assigned to bulk and grain boundary conductivity respectively. The equivalent circuit used to fit the measurement results between 425 °C and 500 °C consists of two ($R//Q$) elements and a Q_{dl} element in series. The latter was necessary in order to fit the measurement results with an equivalent circuit above 400 °C and could be attributed either to the roughness of a blocking electrode or to a non blocking electrode which is smooth and exhibits a Warburg impedance due to the slow diffusion of a reactant species to the interface [19]. The nickel electrodes that are used in the current experiment are blocking to Li^+ ions and therefore the element Q_{dl} must be attributed to the roughness of the electrode–material interface. This 'Warburg element'-like behavior is explained, as different parts of the interface have different bulk resistance pathways, thus causing a transmission-like behavior [19]. It should be noted that, since the low frequency limit of our measurement device is as low as 42 Hz, only the start of a semicircle appears at temperatures 400 °C and 500 °C (Fig. 4), in the low frequency region. This low frequency region corresponds to the right part of the impedance plots. The n-factor in the (rQ) elements that correspond to the bulk and through grain boundaries conductivity mechanisms was found to be very close to 1, almost over the whole temperature range. This close to 1 value of n indicates that these constant phase elements have a strongly capacitive behavior.

The conductivities σ_b, σ_{gb} and σ_{agb} versus temperature diagrams are shown in Fig. 5. The values of these conductivities were calculated from the impedance measurement results as the sample was heated up to 500 °C and then cooled down to 25 °C. In the heating part of the plot from room temperature to about 175 °C and in the cooling part of the plot from about 175 °C to room temperature, a considerable reversible change in bulk conductivity σ_b and grain boundary conductivity σ_{gb} was observed. Specifically, a decrease in conductivity occurred as the material was heated up to 175 °C. This decrease in conductivity is not consistent with ionic conductivity temperature dependence. Similar temperature dependence of conductivity has been observed in the case of $LiNiVO_4$, $LiCoVO_4$ and Li_3VO_4 [10,11]. In these materials it has been shown that this temperature dependence of conductivity can be explained by a reversible absorption–desorption mechanism in the temperature range between 25 °C and 150 °C [11]. As it is shown in the $LiMgVO_4$

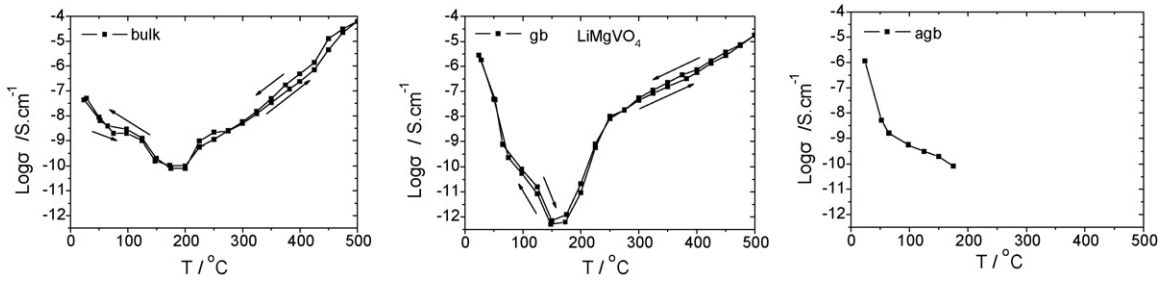

Fig. 5. σ_b, σ_{gb}, σ_{agb} versus temperature plots for $LiMgVO_4$.

TG/DTA measurements (Fig. 6), there is a weight loss of about 2.7% in the temperature range from 25 °C to 200 °C. Similarly to $LiNiVO_4$, $LiCoVO_4$ and Li_3VO_4 this weight loss is attributed to loss of absorbed humidity. As it is shown in Fig. 5, the grain boundary conductivity σ_{gb} decreases seven orders of magnitude as the material is heated up to 200 °C. This major decrease in conductivity is attributed to the fact that the absorbed water forms a humidity film surrounding the grains which causes conductivity along the grain boundaries. The bulk conductivity σ_b decreases only three orders of magnitude as the material is heated up to 200 °C. This smaller decrease in bulk conductivity in comparison with the grain boundary conductivity decrease is attributed to the fact that the absorbed water affects more the boundaries of the grains than their interior. By extrapolating the high temperature part of log(σ) versus T plot for σ_{bulk}, Fig. 5, conductivity becomes very low, about 10^{-13} S.cm^{-1}. As it can be seen comparing $LiNiVO_4$, $LiCoVO_4$ and Li_3VO_4 [10,11] and $LiMgVO_4$ (present work), the conductivity depends on the amount of absorbed water, i.e., the more water is absorbed the more the conductivity changes. In the case of $LiNiVO_4$ and $LiCoVO_4$ the weight loss was 0.8 and 0.5 wt% and the conductivity enhancement 2–3 and 1–2 orders of magnitude, respectively [10]. In Li_3VO_4 a weight loss of 1% results in a difference of 3–4 orders of magnitude [11]. On the other hand, as it is mentioned above, 2.7% weight loss in $LiMgVO_4$ results in difference 3–7 orders of magnitude. We believe that the third process shown in Fig. 5 is strongly related to the weight loss and uptake observed in the TG measurements and reflects a possible protonic conduction mechanism along the grain boundaries, due to surface water absorbed during the heating and the cooling cycle at low temperatures.

The Arrhenius plots of the $LiMgVO_4$ bulk and grain boundary conduction processes are shown in Fig. 7. Their linear behavior shows conductivity processes in accordance with the Arrhenius expression, $\sigma = A\exp(-E_{act}/RT)$. The activation energy is related with the easiness of ion hopping and depends on the crystal structure and in particular on the openness of conduction pathways. In Fig. 7, the bulk conductivity activation energy was calculated to be 0.62 eV**.** The grain boundaries activation energy was calculated to be to be 1.03 eV up to 275 °C and 0.50 eV from 300 °C to 500 °C. This behavior is consistent with defect conduction, with perhaps the low temperature activation energy being related to defect migration only and the higher temperature activation energy being related to migration plus defect creation. According to Lilley and Strutt [20], this could be attributed to the fact that at low temperatures, the along grain boundary conduction is dominated by easy paths, while at high temperatures, transport along the grain boundary overtakes the easy path mechanism.

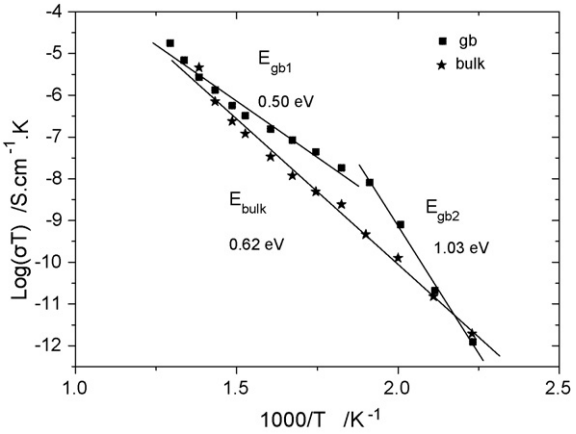

Fig. 7. Arrhenius plots of $LiMgVO_4$ conduction processes and their calculated activation energy values.

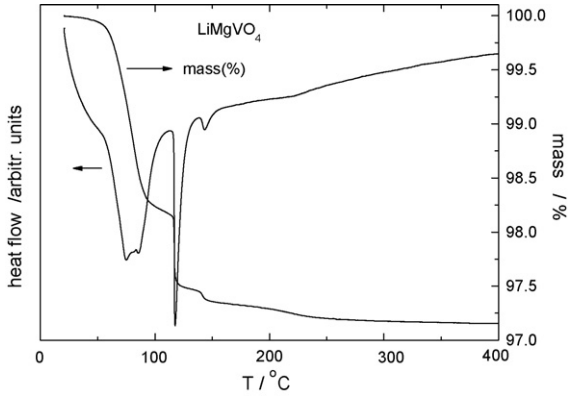

Fig. 6. Mass loss (TG/%) and derivative mass loss (DTG) measurements of $LiMgVO_4$.

4. Conclusions

A study of the conductivity mechanisms of $LiMgVO_4$ in the temperature range of 25–500 °C is presented. This study revealed, for the first time, the drastic effect of humidity on conductivity for this compound in the temperature range of 25–175 °C. It was shown that at each temperature level the real part of the specific conductivity is constant up to a certain frequency. The frequency at which the specific conductivity starts to increase corresponds to the material's hopping frequency at the set temperature. Above the hopping frequency the specific conductivity increases linearly with frequency in the log(σ) versus log(f) plots. At 500 °C, as the material' s hopping frequency is above the maximum frequency of the measurements taken (1 MHz), the real part of the specific impedance is the same at all frequency values within the range of 42 Hz to 1 MHz. The conduction of the material was attributed to three conduction mechanisms. The conduction mechanism through the grains σ_b, the conduction mechanism through the grain boundaries σ_{gb}, and the low temperature conduction mechanism σ_{agb}, that is associated with humidity absorption–desorption. The bulk and grain

boundary conductivities decrease considerably as the material is heated from 25 °C to 175 °C. This decrease in conductivity with increasing temperature is not consistent with pure ionic conductivity and was attributed to the humidity absorption–desorption mechanism. The calculation of the activation energies of the bulk and grain boundary conduction mechanisms was based on the Arrhenius plots. The activation energy of the bulk conductivity was found to be 0.62 eV. In the case of the grain boundary two different activation energy values were calculated. Up to 275 °C a 1.03 eV activation energy value was calculated and, from 300 °C to 500 °C, a 0.50 eV activation energy value was calculated. The results obtained for $LiMgVO_4$, confirm the already published interpretation of the electrical properties of $LiMVO_4$ (M= Ni, Co, Li) [10,11]. An extension of this study on M = Mn, Fe and Zn compounds is in progress. Preliminary results show that the amount of absorbed humidity as well as its effect on the electrical properties depends on the kind of the M cation and on microstructure. A comparative study of all members of this family of materials at different relative humidity atmospheres and the influence of their structure and microstructure as well as of other critical parameters such as material ageing on their conductivity, must be performed in the future in order to further explore their possible use as humidity sensors.

References

[1] G. Blasse, J. Inorg. Nucl. Chem. 25 (1963) 230–231.
[2] A.F. Corsmit, G. Blasse, Chem. Phys. Lett. 20 (1973) 347–349.
[3] M.Th. Paques-Ledent, Chem. Phys. Lett. 24 (1974) 231–233.
[4] M.Th. Paques-Ledent, Chem. Phys. Lett. 35 (1975) 375–378.
[5] D. Capsoni, M. Bini, V. Massarotti, P. Mustarelli, F. Berlotti, P. Galinetto, J. Phys. Chem. B 110 (2006) 5409–5415.
[6] H. Ronde, G. Blasse, J. Inorg. Nucl. Chem. 40 (1978) 215–219.
[7] H. Ronde, J.G. Snijders, Chem. Phys. Lett. 50 (1977) 282–283.
[8] H. Ronde, G. Blasse, J. Solid State Chem. 17 (1976) 339–341.
[9] G.T.K. Fey, D.L. Huang, Electrochim. Acta 45 (1999) 295–314.
[10] A. Kazakopoulos, C. Sarafidis, K. Chrissafis, O. Kalogirou, Solid State Ionics 179 (2008) 1980–1985.
[11] A. Kazakopoulos, O. Kalogirou, J. Mater. Sci. 44 (2009) 4987–4992.
[12] A. Kazakopoulos, O. Kalogirou, Solid State Ionics 179 (2008) 936–940.
[13] Y. Yokomizo, S. Uno, M. Harata, H. Hiraki, K. Yuki, Sens. Actuatators 4 (1983) 599–606.
[14] M.T. Wu, H.T. Sun, P. Li, Sens. Actuatators B-Chem. 17 (1994) 109–112.
[15] J.R. Ying, C.R. Wan, P.J. He, Sens. Actuatators B-Chem. 62 (2000) 165–170.
[16] A.R. West, in: G. Peter, Bruce (Eds.), Solid State Electrochemistry, Cambridge University Press, 1995, p. 22.
[17] Bernard A. Boukamp, Equivalent Circuit (EQUIVCRT.PAS), University of Twente (1989).
[18] N. Bonanos, B.C.H. Steele, E.P. Butler, in: E. Barsoukov, J.R. Mackdonald (Eds.), Impedance Spectroscopy, J. Wiley & Sons, 2005, pp. 205–264.
[19] A.R. West, in: G. Peter, Bruce (Eds.), Solid State Electrochemistry, Cambridge University Press, 1995, p. 228.
[20] E. Lilley, J.E. Strutt, Phys. Status Solidi A 54 (1979) 639–650.